

Nanodomain stabilization dynamics in plasma membranes of biological cellsTamal Das,¹ Tapas K. Maiti,¹ and Suman Chakraborty^{2,*}¹*Department of Biotechnology, Indian Institute of Technology, Kharagpur 721302, India*²*Department of Mechanical Engineering, Indian Institute of Technology, Kharagpur 721302, India*

(Received 7 June 2010; revised manuscript received 25 November 2010; published 16 February 2011)

We discover that a synergistically amplifying role of stabilizing membrane proteins and continuous lipid recycling can explain the physics governing the stability, polydispersity, and dynamics of lipid raft domains in plasma membranes of biological cells. We establish the conjecture using a generalized order parameter based on theoretical formalism, endorsed by detailed scaling arguments and domain mapping. Quantitative agreements with morphological distributions of raft complexes, as obtained from Förster resonance energy transfer based visualization, support the present theoretical conjecture.

DOI: [10.1103/PhysRevE.83.021909](https://doi.org/10.1103/PhysRevE.83.021909)

PACS number(s): 87.16.dt

I. INTRODUCTION

The physics of phase separation in cell membranes has given rise to many unresolved apparent anomalies, primarily attributable to nontrivial dependences of the underlying nanodomain dynamics on the spatiotemporal responses of the included macromolecules such as lipids and proteins against an imposed perturbation, as well as a complex auto-organization process dictating the membrane functionalities [1,2]. On well-addressable physical scales *in vivo*, these phenomena have often been ascribed to the formation of lipid rafts, which are believed to be [1] nanometer sized “less fluidic” domains, enriched with cholesterol, sphingolipids, and specific membrane proteins. These raft elements are engulfed within a “more fluidic” bulk phase of unsaturated lipids [Fig. 1(a)] [2] and effectively control several critical and specialized functionalities, including signals transductions, sensing, and sorting of proteins [1,2].

From elementary considerations of thermodynamic stabilities, it is expected that the saturated (or unsaturated) portions of the matrix are likely to constitute single separated bulk phases [2,3], rather than forming multiple submicron domains. Nevertheless, the experimental outcomes confirm the latter [2,4,5]. Preliminary studies from the researchers have attributed the length-scale limitation to a possible persistent nonequilibrium recycling of the raft elements [6–9]. Further, practical investigations have emphasized on additional contributions of lipid-protein interactions toward the raft domain formation [1,5].

As indicated from the reported literature, the role of membrane proteins in nanoscale lipid raft formation can be bimechanistic. On one hand, membrane proteins have been realized to act as surfactant molecules, reducing the interfacial tension between ordered and disordered lipid domains. On the other side, there are propositions that sparsely distributed membrane proteins may nucleate raft nanodomains. Importantly, while there are ample substantiations that specific protein conformations do indeed link between the tails of saturated and unsaturated fatty acids and consequently, these proteins are partitioned into the lipid ordered and disordered domain boundary, the second mechanism remains

controversial from a detailed structural viewpoint. The major criticisms of the nucleation hypothesis originate from its predictions related to the raft growth with the decreasing temperature and the imparted dominating role of the membrane proteins [2]. Within the framework of protein-lipid interaction, which occurs essentially through short-ranged attraction (by homophilic interaction or depletion effect) and long-ranged repulsion (by steric or electrostatic interaction), the formation of lipid raft aggregates are expected to be governed solely by the distribution of predisposed membrane proteins. In the literature, this is referred to as the “passive” mechanism of the raft formation where membrane lipids are to be satisfied with a “secondary” role. However, as probed experimentally, the lipid raft dynamics, at least in live cells, should not be governed by a passive mechanism [5]. Rather, a more active mode of interaction, as portrayed by the “pinning” or “surfactant” hypothesis, should be invoked to reproduce the reality.

Moreover, from the nucleation hypothesis, it can be inferred that the width of the lipid raft band around a nucleating protein molecule should be of the order of the correlation length of the phase-separating system. In ambient environments, the system is assumed to exist above its critical temperature in which the spontaneous lipid separation occurs. Subsequently, if the temperature is decreased toward the critical value then the correlation length should diverge, increasing the associated lipid bandwidth. As the protein-protein attractive interaction is expected to span over the lipid bandwidth (i.e., proteins whose lipid bands overlaps attract each other), the decreasing system temperature will imply progressively larger membrane protein clusters [2]. However, in contrast to the aforementioned anticipation, the membrane protein clusters have not been observed to grow significantly with the decreasing temperature, at least within the permissible range.

On the contrary, the interface “pinning” by a “surfactant” mechanism enables a more dynamic and realistic depiction of the membrane nanodomain formation. It is generally recognized that while the “core raft connectivity” is established by the sphingolipid-cholesterol assemblage potential, the dynamics of nanodomain formation can be significantly influenced by the protein specificity [1]. It has been known for a long time that there are specific proteins which can form favorable linkages with both saturated and unsaturated fatty acid tails by means of different interaction domains within the same amino-acid chain. It is then expected that these will be preferentially

*suman@mech.iitkgp.ernet.in

located in the saturated-unsaturated lipid interface and should reduce the effective critical temperature for phase separation. Hence, though the pure mixture undergoes complete phase separation at physiological temperature, this is prevented in the cell plasma membrane due to the presence of surfactant proteins. To date, only the immobilized protein model has been employed in this context, and importantly, Fan *et al.* have demonstrated that “pinning” of interfaces with immobile proteins can stabilize raft nanodomains over a macroscopic time scale [2]. However, the aforementioned pinning and stabilizing effects are expected to be decimated drastically if, instead of immobility, finite diffusion of the surfactant protein is allowed [2]. Also to effectuate nanoscopic raft sizes within the “immobilized” paradigm, the membrane protein density has to be abnormally high [2]. To eliminate the aforementioned drawbacks of the “pinning” hypothesis, we employ a more realistic mobile protein model and illustrate how the synergistic interaction between the surfactant and recycling mechanism can form stable nanodomains, even if the membrane proteins are endowed with finite diffusivity. It is compelling to note that subsequent to “fixing” the chemical modification of proteins such as formaldehyde and thiol treatments, which eliminate the mobility of membrane proteins, phase separation in the plasma membrane increases in length scale [1]. This behavior is well explained from the interface “pinning” hypothesis, which indeed predicts the increase in domain length scale with the reduced protein mobility [2]. However, this emerges to be inconsistent with the presumed consequences of nucleation proposition where finite protein mobility enables the agglomeration of separately nucleated clusters. These, in summation, instigate us to select the first mechanism as the dominating influence of the membrane proteins in lipid raft nanodomain formation. Although there are definite possibilities that the nucleation process can be equally influential in raft-domain organization, as the interface pinning mechanism is, we have included the surfactant mechanism in the present model as the predominating role of membrane proteins, relying on the growing evidence in favor of the latter.

Following the above discussions, it may be conjectured that the raft domain formation may be perceived to be a combined consequence of the lipid raft recycling process and the lipid-protein interaction mechanisms. However, the physics of such interactions, particularly in pertinence with the observed topographical features and length scales of the plasma membrane heterogeneities, has, to date, remained to be rather elusive from both the theoretical and experimental perspectives [2]. As highlighted recently [2], the combined influence of coexisting mechanisms can be extremely non-trivial in guiding the ultimate raft domain dynamics. In this relevance, it is pertinent to mention that while Fan *et al.* [2] examined the dynamics of structure factor by considering five possible mechanisms including pinning and recycling, they raised an important question—*what is the effect of interaction between the pinning and recycle processes if both of these are considered to be occurring simultaneously?* As it appears, the interaction between the lipids and membrane protein, in the process of raft domain formation, is more of a dynamic in nature, in contrast to existing “passive protein” models and therefore, may have a nonintuitive relation with the nonequilibrium recycling kinetics.

Here what we propose is believed to be the first model of plasma membrane heterogeneity investigating the effect of concomitant interface pinning and recycling mechanisms, supported by direct experimental evidence and based on the synergistic dynamical interactions between lipid raft recycling phenomenon and surfactant/wetting [1,2] effects of membrane proteins. With a free-energy-derived phase-field model describing the coupled temporal variation of an order parameter representing the fraction of raft elements and a density parameter for protein molecules, we quantitatively delineate the relative contribution and synergistic interaction between the surfactant effect and the recycling process toward generating an exclusively diverse array of polydisperse raft domains in the form of a lipid raft complex. Within this framework, we are able to delineate the process from a tractable computational level [2] and to retain provisions for protein mobility [2]. Using a perturbation method along with scaling arguments, we uniquely demonstrate the dynamic role of the membrane protein [2] in raft stabilization [7–9]. From an experimental perspective, we map the dynamical evolution of the raft domains *in vivo*, employing a Förster resonance energy transfer (FRET) [3] based raft visualization technique, and corroborate our theoretical findings with the experimental trends.

II. MODEL

The plasma membrane may be conceptualized as a two-component fluid where the lipids are categorized into two major classes, namely saturated (S) and unsaturated (U). In a two-dimensional framework, we define a phase-field variable $\phi(r) = n_S(r)/n_0$, where n_0 is the total lipid density [8] and $n_S(r)$ is the surface density of saturated lipid classes (rafts). In this way, ϕ varies from unity in the saturated domain to zero in the unsaturated domain. We further consider that membrane proteins (having relative surface density ρ with respect to its saturation value ρ_s) behave like surfactant molecules and mostly cluster into the raft-unsaturated lipid interfaces. Considering this, we model the free energy of the system as a function of both ϕ and ρ .

$$F(\phi, \rho) = \int d^2r \left[f(\phi) + \frac{\kappa^2}{2} (\nabla\phi)^2 + e\rho^2(\rho - \rho_s)^2 - \rho^2[g_1(1 - \phi)^2 + g_2\phi^2] - \sigma\rho(\nabla\phi)^2 \right]. \quad (1)$$

In Eq. (1), the first two terms arise from the classical description of free energy of mixing and interphase interfacial energy, respectively. The former can be expressed as $f(\phi) = \phi \ln \phi + (1 - \phi) \ln(1 - \phi) + \chi\phi(1 - \phi)$, where χ is a lipid-lipid interaction parameter [8]. The last three terms in Eq. (1) account for the surfactant effect of the protein molecules [10,11]. In this physical description, the saturation concentration (ρ_s) acts like a double-well potential and effectively ensures the coexistence of neighboring dilute and concentrated protein phases [11]. The condition $\sigma \gg g_1, g_2$ ensures the experimentally illustrated accumulation of proteins in the S - U interface, which, in turn, stabilizes the raft domains by eliminating the interfacial tension in the limit of saturated protein concentration (ρ_s) at the S - U boundary. This limiting condition may be achieved if the

following relationship holds: $\sigma = \kappa^2/2\rho_s$. The dynamical evolution of the phase-field parameter and the relative density parameter may be dictated by the following evolution equations: $\frac{\partial\phi}{\partial t} = M_\phi \nabla^2 \frac{\delta F}{\delta\phi} + R_\phi + \eta_\phi(r,t)$, and $\frac{\partial\rho}{\partial t} = M_\rho \nabla^2 \frac{\delta F}{\delta\rho} + \eta_\rho(r,t)$. Here, $M_{\phi(\rho)}$ is the mobility parameter of $\phi(\rho)$, and $\eta_{\phi(\rho)}(r,t)$ is a stochastic contribution of the following form: $\langle \eta_{\phi(\rho)}(r,t) \eta_{\phi(\rho)}(r',t') \rangle = 2M_{\phi(\rho)} k_B T \delta(r-r') \delta(t-t')$. Here, a reaction term $R_\phi = -(\phi - \bar{\phi})/\tau_R$ arises from the recycling of raft elements [8] between the membrane and golgi complex, demarcating a “live” cell from an inanimate vesicle. τ_R is the typical recycling time and ranges within 10–15 minutes. The ensemble-averaged domain size $\langle r(t) \rangle$ at each simulation step is determined as the inverse of the first moment of the structure factor $S(k,t)$ where ϕ_{k_x,k_y} is two dimensional fourier transform of $\phi(x,y)$ and $S(k,t) = \langle |\phi_{k,k}(t)|^2 \rangle$ [12]. The dispersity parameter, which is a quantitative depiction of domain-size diversity, is given by $\delta(t) = |(\sum_k k S(k,t))^2 - \sum_k k^2 S(k,t)|^{0.5} / \sum_k k S(k,t)$. Henceforth, δ denotes domain dispersity at the steady-state condition ($t \rightarrow \infty$). The above evolution equations are nondimensionalized with respect to a characteristic time scale $\tau = \kappa^2/M_\phi a^2$ and length scale $\lambda = \kappa/\sqrt{2a}$, where $a = 2(2 - \chi); a > 0$. Other simulation parameters are taken as [8,13] $\kappa = 1\text{nm}$, $M_\phi = 10^{-12}\text{m}^2\text{s}^{-1}$, $a = 1$, $\phi_0 = 0.3$, and $M_\rho = M_\phi$, if not otherwise specified. With these values, $\tau \sim 1\mu\text{s}; \lambda \sim 0.707\text{nm}$. Considering the experimentally observed recycling time (in minutes) [6], the basal recycling rate is chosen such that $\tau_R^0 = 10^8\tau$. The governing transport equations are discretized in $(2+1)$ -dimensional space-time following a finite-difference scheme, with time step size of $\Delta\tau = 0.001\tau$ and grid spacing $\Delta x = \Delta y = \lambda$ in a domain of 1024×1024 grids, along with periodic boundary conditions. This eliminates the finite-size effect. Throughout the text, we have used $\langle r \rangle$ to represent the ensemble-averaged domain size at any time step while $\langle r_{ss} \rangle$ or $\langle \Pi \rangle$ have been used to denote the ensemble-averaged steady-state domain size in the limit of $t \rightarrow \infty$. The initial protein density has been assigned to be uniform at all grid points and is represented by ρ_0 . With time, though the spatial distribution changes following the governing equation, the ensemble averaged density over all grid points ($\langle \bar{\rho} \rangle$) remains fixed to ρ_0 .

III. MATERIALS AND METHODS

To experimentally visualize the raft domains in living cells, FRET imaging is appreciated to be the most elegant [1,3]. Here, we have augmented the resolution power of FRET in tune with a single molecule imaging technique [14] to capture the essential domain dynamics. First, we have labeled HeLa (representative human cell-line, cervical carcinoma origin) cells with carbocyanine FRET pair dyes (DiOC₁₈ and DiIC₁₈, Sigma, USA, 2 μM in cell culture medium, 30 min incubation at 37°C), which are preferentially partitioned into a cholesterol-rich lipid raft domain. In effect, high-intensity FRET emission is expected to be exclusively on raft locations [3]. For measurements, images have been captured at acceptor (excitation: 543 nm, emission: 550–630 nm), donor (ex: 488 nm, em: 500–540 nm), and FRET (ex: 488 nm, em: 550–630 nm) specific wavelengths. FRET at each point is estimated by an existing protocol [14]. These domains then

have been imaged using a single molecule tracking confocal technique with a submicron resolution [14]. This has been obtained employing a fast scan speed (65 ms per frame, round-trip model, Olympus Fluoview1000) and blind deconvolution algorithm [15]. Images have been acquired in the photon-count mode to avoid undesired noises. The fact that a single-step bleaching of the fluorescence can be accomplished has ensured the high resolution (i.e., near single molecule) of the captured images [16]. To quantitate the effective FRET, we have determined the donor fluorescence (DiO) quenching due to the presence of energy transfer acceptor (DiI) [17]. First, in the presence of acceptor DiI, an image of DiO fluorescence (DiO_{PRE}) has been acquired. DiI then has been subjected to irreversible photobleaching by extended exposure (normally 5 s) to a scanning laser beam. An image of DiI fluorescence has been acquired to ascertain complete photobleaching of the acceptor. Subsequently, in this condition, in the absence of acceptor fluorescence, an image of DiO in the same field or region of interest (RoI) as previous has been acquired (DiO_{POST}). After subtracting the background from each of the aforementioned images in the same RoI or field, at each pixel of RoI, resonance energy transfer efficiency has been determined as $I_{\text{FRET}}(x,y) = (DiO_{\text{POST}} - DiO_{\text{PRE}})/DiO_{\text{POST}}$. This has ensured $I_{\text{FRET}}(x,y)$ to be within the range between 0 (no FRET as in the phospholipid layer) to 1 (high FRET as in the raft domain). From the FRET images, the structure factor, domain size, and dispersity parameters have been determined using identical formulation as utilized in the theoretical model described above, replacing ϕ by pixel transfer efficiency [$I_{\text{FRET}}(x,y)$] values [15].

IV. RESULTS AND DISCUSSION

A. Domain growth arrest

Without recycling and surfactant effects, the “free growth” leads to a classical coarsening process with conserved phase field parameter [Fig. 1(b)]. However, incorporating a recycling term in the dynamic equation of ϕ incurs a counter-homogenizing effect, leading to a possible domain growth arrest [8]. Given that the time for domain formation (τ_d) is proportional to the cube of domain size, the domain arrest favorably takes place in the limit $\tau_d > \tau_R$, yielding a relation $\langle \Pi \rangle \sim (M_\phi \kappa \tau_R)^{1/3}$ [Fig. 1(b)] and Zone I of Fig. 2(a), where $\langle \Pi \rangle = \langle r_{ss} \rangle$ is the average steady-state or stationary-state domain size. With $\tau_R = \tau_R^0$, raft domains of a size larger than 400 nm are formed with the considerations of recycling without surfactant effects, which is phenomenologically inconsistent. Next, we consider the surfactant effect without recycling. Due to the perturbations in the surfactant distribution over the initial transients, interfaces with both saturated ($\rho \geq \rho_s$) and unsaturated ($\rho < \rho_s$) domains coexist and the domain growth is exclusively arrested at the saturated segments. With time, however, the fraction of interfacial zone with surfactant saturation increases until a nullification of the interfacial tension stabilizes the domain formation to a steady-state distribution [Fig. 1(b)]. From this perspective, the scaling relation $\langle \Pi \rangle (M_\phi \kappa \tau_s)^{1/3}$ should be approximately valid, where τ_s is the time required to attain complete surfactant saturation at the interface. Considering $\tau_s \sim (\rho_s - \rho_0)^3$, we obtain

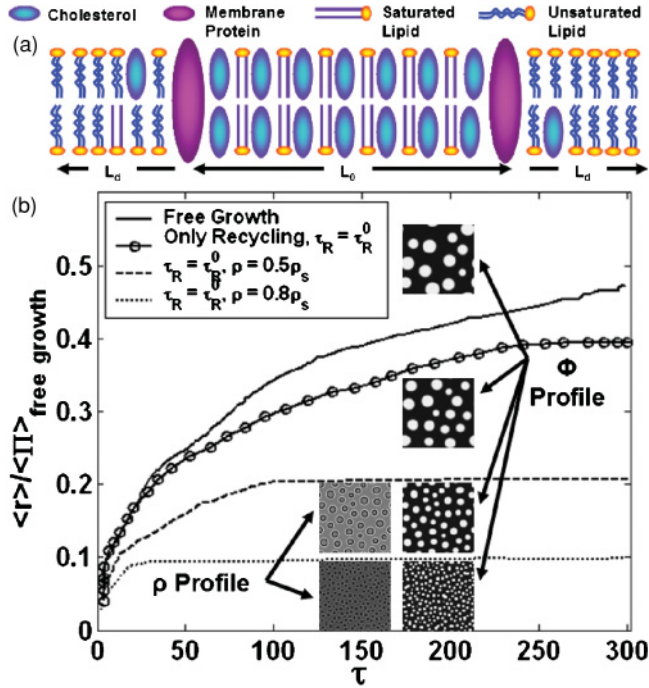


FIG. 1. (Color online) (a) Schematic representation of lipid ordered (raft) and disordered domains of cell membrane. (b) Progressive arrest of domain growth by recycling ($\tau_R = \tau_R^0$) and surfactant effect of membrane proteins (with $\rho_0 = 0.5\rho_s$ and $0.8\rho_s$). Average domain perimeter values are normalized by the $\langle r \rangle$ value corresponding to a complete phase separation in the free growth case. ϕ and ρ profile image shots are given for $t = 200\tau$. Data averaged over at least 20 ensembles.

$\langle \Pi \rangle \sim (\rho_s - \rho_0)$, congruent with the foregoing predictions [11]. However, for $\rho_0 > 0.7$, the simulation results reveal $\langle \Pi \rangle \sim (\rho_s - \rho_0)^{4/3}$ [zone III of Fig. 2(a)]. Since local attainment of saturation density (due to the initial perturbation in ρ) promptly arrests the domain growth, an essential element of localized dimensional polydispersity is in-built into the nanodomain formation mechanism.

We then observe a nonintuitive synergistic functional reinforcement of the domain growth, when two mechanisms act in tandem over zone II [see Fig. 2(a)], and the result is expressed in terms of a scaling relationship of the following form: $\langle \Pi \rangle \sim (\tau_R / \tau_R^0)^\alpha (\rho_s - \rho_0)^\beta$. For the

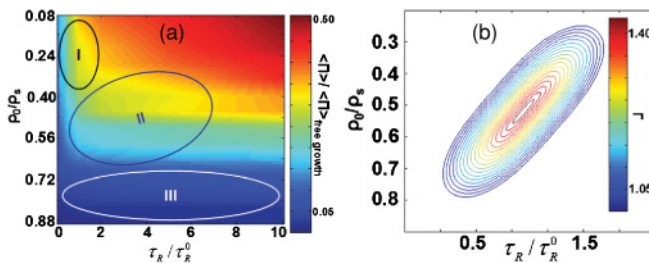


FIG. 2. (Color online) (a) Variation of steady-state domain size ($\langle \Pi \rangle$) with recycling parameter (τ_R / τ_R^0) and normalized initial concentration of membrane protein (ρ_0 / ρ_s). Both recycling and surfactant effects have been considered (b) Contour map of the parameter Γ in the regime where $\Gamma > 1$.

domain defined by $0.8 < \tau_R / \tau_R^0 < 1.5$; $0.5 < \rho_0 / \rho_s < 0.7$, our simulation results reveal $\alpha > 1/3$; $\beta > 4/3$. This implies that the combined consequence of the recycling effects (manifested in terms of variations in τ_R) and surfactant effects (manifested in terms of variations in ρ) amplifies the strength of each of the individual effects when considered simultaneously. Further, over this domain of dual control, $|\Delta \Pi(\rho \rightarrow \rho \pm \delta\rho; \tau_R \rightarrow \tau_R \mp \delta\tau_R)| > |\Delta \Pi(\rho \rightarrow \rho \pm \delta\rho)| + |\Delta \Pi(\tau_R \rightarrow \tau_R \mp \delta\tau_R)|$ (i.e., the conjoint variation is greater than the sum of the individual variations in the average steady-state domain size). To delineate this quantitatively, we define a parameter $\Gamma = \Delta \Pi(\rho \rightarrow \rho - \delta\rho; \tau_R \rightarrow \tau_R + \delta\tau_R) / (\frac{\partial \Pi}{\partial \tau_R} \delta\tau_R - \frac{\partial \Pi}{\partial \rho} \delta\rho)$ such that $\Gamma > 1$ signifies the regime of the synergistic effect [Fig. 2(b)] of the two influencing factors. Appreciating the practical implications of the operating regime [5,6], such trends essentially manifest the emerging synergy in a biomechanistic control and explicate why such organization is naturally selected in an energy efficient system such as a biological cell.

B. Protein mobility and polydispersity

In the regulation of membrane nanodomain dynamics, protein mobility can be an important parameter [2,13]. It is evident (Fig. 3) that over the regime $0.3 < \rho_0 / \rho_s < 0.7$, a reduction in M'_ρ appreciably facilitates larger domain formation. Polydispersity can be infused with the surfactant effect. For a constant recycling rate, the steady-state dispersity parameter (δ) increases to its maximum magnitude at around $\rho_0 = (0.65 \pm 0.04)\rho_s$, as obtained from our simulations, (Fig. 3 inset), which agrees well with the experimentally obtained value of $\delta = 0.6375 \pm 0.1392$.

C. Experimental assessment of domain growth predictions

Given that lipid vesicles recycle along the microtubular tracks with the aid of adenosine triphosphate (ATP) driven

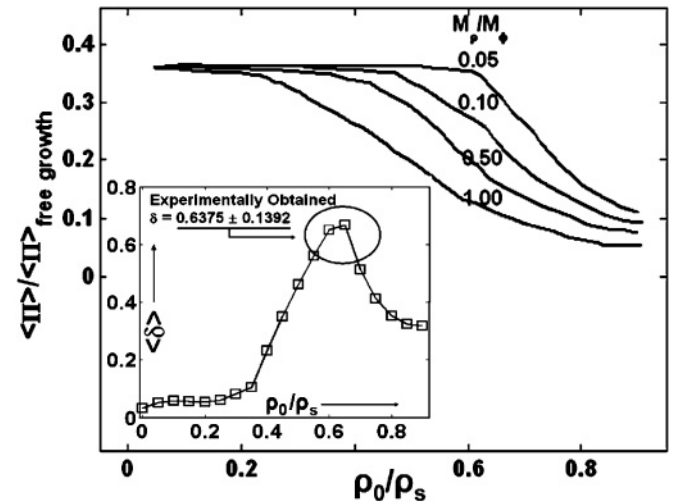


FIG. 3. Variation of steady-state domain length scale with initial membrane protein density depends on the relative mobility (M'_ρ / M_ϕ). (Inset) Dependence of dispersity (δ) on initial membrane protein density. $\tau_R = \tau_R^0$ for all data points.

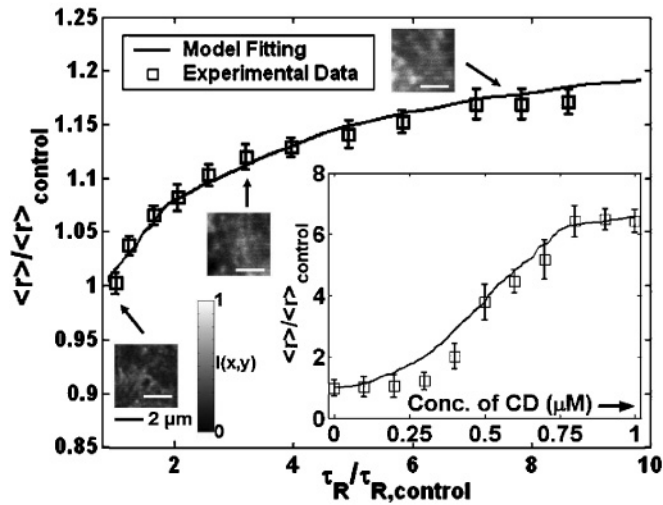


FIG. 4. Comparison of model prediction with experimental data (see main text). We have obtained $\tau_{R,\text{control}} = 1.023\tau_R^0$ and model fitting has been done with $\rho_0 = 0.657\rho_s$. (Inset) $\langle r \rangle$ growth with Cytochalasin D (CD) treatment. We have assumed complete disruption of actin fences with $1\mu\text{M}$ CD. $\tau_R = \tau_{R,\text{control}}$. Number of samples per data point > 5 .

molecular motors [6], to retard the energetic recycling process we have used the ATP-inhibition method [6] with different concentrations (1–10 mM) of an ATP-depleting reagent comprising of sodium azide and deoxy-glucose in a 1:1 v/v ratio. Then, performing simultaneous raft recycling kinetics assay [6] and FRET intensity domain analysis, a reasonable congruency has been achieved between model speculations and experimental observations for different values of the recycling time (Fig. 4). For this analysis we have normalized the experimentally observed recycling times and domain size parameters with their corresponding values ($\tau_{R,\text{control}}$ and $\langle r \rangle_{\text{control}}$, respectively) from control (without treatment) samples. Identical normalization has been imposed on theoretically obtained values to preserve the consistency of comparison. As anticipated, the profile of domain size against the varying recycling times differs for different presumed initial protein densities (i.e., for different magnitudes of ρ_0). However, the least mean-square fit between experimental and model trends has been obtained for $\rho_0 = 0.657\rho_s$, which falls in the range of the anticipated protein density. In the absence of practical knowledge about the actual surfactant protein concentration in the plasma membrane *in vivo*, we propose this value to be the logical approximation of the membrane surfactant protein density, which has been, subsequently, used in the following comparative investigations.

Toward the other end of the parametric spectrum, we have attempted to experimentally elucidate the influence of membrane protein concentration on nanodomain dynamics. Here the most vital and related concept is that the abundance of surfactant proteins, and simultaneously their role in raft stabilization, depends upon the presence of cortical (beneath the plasma membrane) cytoskeletal elements [1]. To appreciate this fully, it should be reviewed that the lipid rafts are perceived to be organized by lipids such as

cholesterol, glycosphingolipids, and polyphosphoinositides, especially PIP_2 [1]. While the “core raft connectivity” is due to the sphingolipid-cholesterol assemblage potential, the membrane nanoheterogeneity can be dictated by the protein specificity [1]. The relevant proteins in this regard are mostly transmembrane (TM) ones which either link PIP_2 and cortical actin or glycosylphosphatidylinositol-anchored (GPI-anchored) proteins and cortical actin [1]. In both ways the cortical actin has been probed to play an important role in providing the protein-induced modifications of the raft structure. To substantiate, a recent study has uncovered a TM protein (carboxy-terminal Src kinase or Csk-binding protein, i.e., CBP) which forms linkages between the GPI-anchored protein Thy-1 and the cortical cytoskeleton via another mediating protein called EBP50-ERM [19]. While both CBP and Thy-1 have been identified to be involved in lipid-protein mediated signaling events and are preferentially raft partitioned, the TM protein CBP has been envisaged to have an additional role of organizing membrane nanoheterogeneity [1,19]. Moreover, the transient lateral confinement of GPI-anchored proteins, presumably due to entrapment in raft domains, has often been observed to depend crucially upon the existence of cortical actin filaments [1,18]. It is then inferred that cortical actin complexes impart a decisive influence in the organization of sphingolipid-cholesterol-enriched lipid raft domains, mostly by providing a scaffold for the TM proteins that do exhibit the necessary attributes for “wetting” lipid ordered-disordered interfaces [1]. It is again very compelling to note that *in vivo* raft-associated TM proteins are excluded from the lipid-ordered phases not only in reconstituted model membranes, but also in giant vesicles formed by promoting the blebbing of physiological plasma membrane [1]. As the latter is expected to be almost chemically invariant as compared to the functional plasma membrane and has been widely used as the near-exact model in immunological studies, the fact that TM proteins partition differently points out the imperative role of nonmembrane elements such as the cortical cytoskeleton. It is then anticipated that the linkage of TM proteins with cortical actin filaments mediates the necessary structural alternations in TM domains, which confers the specific surfactant characteristics. These background inferences have inspired us to disrupt the cortical actin structure with an actin filament depolymerising drug such as Cytochalasin D (CD) to probe the effect of surfactant proteins on raft organization, as followed by the theoretical predictions.

Accordingly, in principle, we suppose that the complete disruption of the actin cytoskeleton, as implemented by treating cells with $1\mu\text{M}$ of CD, would correspond to $\rho_0 = 0$, while the control should stand for $\rho_0 = 0.657\rho_s$, as approximated above. With this consideration, the model predictions closely match with the experimentally probed $\langle r \rangle$ values (Fig. 4 inset). Related to the proposed synergy, the effect of the combined treatment with $0.1\mu\text{M}$ of CD and 1 mM ATP-depleting reagent $\Delta r^* = \Delta r / \langle r \rangle_{\text{control}} = 0.2149 \pm 0.0527$ is significantly greater than the sum of the individual effects ($\Delta r_{0.1\mu\text{M CD}}^* = 0.0369 \pm 0.0092$; $\Delta r_{1\text{mM dATP}}^* = 0.0372 \pm 0.0119$). This trend is maintained for 0.1–0.3 μM of CD and 1–2 mM ATP-depleting reagent as well.

V. CONCLUSION

In this investigation we have theoretically and experimentally demonstrated that an intricate bidirectional interaction between the lipid raft recycling mechanism and surfactant effect of membrane proteins, over certain regimes, may implicate a synergistic amplification of growth arresting kinetics of the polydisperse lipid raft subdomains. This essentially favors the dynamic lipid-protein interaction model, as emergent in

recent investigations [2,13], rather than protein molecules partitioning into pre-existing rafts. Given the implications of the results and the fact that our study consummates the hitherto missing direct correspondence between the theoretical and experimental findings related to lipid raft stabilization [2], we expect it to incite further inquiries concerning the origin and evolution of raft nanodomains from a more detailed biophysical perspective.

-
- [1] D. Lingwood and K. Simons, *Science* **327**, 46 (2010); J. F. Hancock, *Nat. Rev. Mol. Cell Biol.* **7**, 456 (2006); S. Munro, *Cell* **115**, 377 (2003); L. J. Pike, *J. Lipid Res.* **44**, 655 (2003); R. F. de Almeida *et al.*, *J. Mol. Biol.* **346**, 1109 (2005).
- [2] J. Fan, M. Sammalkorpi, and M. Haataja, *Phys. Rev. Lett.* **104**, 118101 (2010); *FEBS Lett.* **584**, 1678 (2010).
- [3] K. Gaus *et al.*, *Proc. Natl. Acad. Sci. USA* **100**, 15554 (2003); M. Rao and S. Mayor, *Biochim. Biophys. Acta* **1746**, 221 (2005).
- [4] C. Dietrich *et al.*, *Biophys. J.* **80**, 1417 (2001); N. Kahya, D. A. Brown, and P. Schwille, *Biochemistry* **44**, 7479 (2005); S. L. Veatch and S. L. Keller, *Phys. Rev. Lett.* **89**, 268101 (2002).
- [5] H.-J. Kaiser *et al.*, *Proc. Natl. Acad. Sci. USA* **106**, 16645 (2009).
- [6] B. J. Nichols *et al.*, *J. Cell Biol.* **153**, 529 (2001).
- [7] M. S. Turner, P. Sens, and N. D. Socci, *Phys. Rev. Lett.* **95**, 168301 (2005).
- [8] L. Foret, *Europhys. Lett.* **71**, 508 (2005).
- [9] J. Fan, M. Sammalkorpi, and M. Haataja, *Phys. Rev. Lett.* **100**, 178102 (2008); J. Gómez, F. Sagués, and R. Reigada, *Phys. Rev. E* **77**, 021907 (2008); **80**, 011920 (2009).
- [10] P. C. Hohenberg and B. I. Halperin, *Rev. Mod. Phys.* **49**, 435 (1977).
- [11] S. Komura and H. Kodama, *Phys. Rev. E* **55**, 1722 (1997); M. Laradji, H. Guo, M. Grant, and M. J. Zuckermann, *Phys. Rev. A* **44**, 8184 (1991).
- [12] S. C. Glotzer, E. A. Di Marzio, and M. Muthukumar, *Phys. Rev. Lett.* **74**, 2034 (1995).
- [13] S. J. Plowman, C. Munke, R. G. Parton, and J. F. Hancock, *Proc. Natl. Acad. Sci.* **102**, 15500 (2005).
- [14] R. Roy, S. Hohng, and T. Ha, *Nat. Methods* **5**, 507 (2008); Z. Xia and Y. Liu, *Biophys. J.* **81**, 2395 (2001).
- [15] V. Vukojević *et al.*, *Proc. Natl. Acad. Sci.* **105**, 18176 (2008); S. L. Veatch *et al.*, *ACS Chem. Biol.* **3**, 287 (2008).
- [16] G. M. J. Segers-Nolten *et al.*, *Nucleic Acid Res.* **30**, 4720 (2002).
- [17] A. K. Kenworthy, N. Petranova, and M. Edidin, *Mol. Biol. Cell* **11**, 1645 (2000).
- [18] K. G. Suzuki *et al.*, *J. Cell Biol.* **177**, 717 (2007); D. Goswami *et al.*, *Cell* **135**, 1085 (2008).
- [19] Y. Chen, L. Veracini, C. Benistant, and K. Jacobson, *J. Cell Sci.* **122**, 3966 (2009).